



Midnight Sun Solar Car Team
University of Waterloo

Preliminary Vehicle Design Report

MSXII

Prepared by:
Minghao Ji
minghao.ji@uwmidsun.com
October 16, 2017

Contents

1	History	2
2	Contacts	3
3	Mechanical	3
3.1	Overview	3
3.2	Chassis	3
3.2.1	Design	3
3.2.2	Manufacturing	3
3.2.3	Roll cage	3
3.3	Seat belts	8
3.4	Braking system	8
3.4.1	Primary brakes	8
3.4.2	Parking brake	8
3.5	Steering system	11
3.6	Suspension	11
3.6.1	Front suspension	11
3.6.2	Rear suspension	11
3.7	Finite element analysis	11
3.7.1	Front suspension	13
3.7.2	Rear suspension	14
3.7.3	Steering	14
3.7.4	Results	14
4	Electrical	15
4.1	Overview	15
4.2	Battery	15
4.2.1	Testing Methodology	16
A	Loading conditions	18
A.1	Braking	18
A.2	Acceleration	18
A.3	Cornering	19
A.4	Bump	20
A.5	Superposition	20
A.6	Summary	21
B	FEA images for chassis	23
C	FEA images for suspension and steering	28

List of Figures

1	Top view showing major dimensions and system positions	4
2	Side view showing major dimensions and system positions	5
3	Chassis, front view	5
4	Chassis, top view	6
5	Chassis, side view	6
6	Welding jig on rotating mount	7
7	Chassis with roll cage elements highlighted	7
8	Chassis mounting points for seat belts	8
9	Single seat belt tab	9
10	Side view of seat belt geometry	9
11	Top view of seat belt geometry	10

12	Schematic of primary braking system	10
13	View of dual-primary calipers and parking caliper on front suspension upright	11
14	View of steering assembly	12
15	View of front suspension assembly (parking brake caliper obstructed by hub)	12
16	View of rear suspension assembly	13
17	Block diagram of all electrical systems	15
18	Block diagram of all high-voltage electrical systems	16
19	Free body diagram of vehicle braking	19
20	Free Body Diagram of a Car Cornering	20
21	Suspension coordinate system	22
22	Front bumper collision	23
23	Front bumper 30 degree collision	23
24	Front bumper 60 degree collision	23
25	Side bumper collision	24
26	Rear bumper collision	24
27	Hood 60 degree collision	24
28	Hood 30 degree collision	24
29	Side 60 degree collision	25
30	Side 30 degree collision	25
31	Roof top collision	25
32	Vehicle rest front subframe loading	25
33	Vehicle rest front subframe stress	26
34	Vehicle rest rear subframe stress	26
35	Torsion test, deformation	26
36	Torsion test, stress	27
37	Coilover clevis	28
38	Upper control arm	28
39	Lower control arm	28
40	Upright	29
41	Spindle	29
42	Upper control arm clevis	29
43	Upper bearing plate	30
44	Coilover mounting plate	30
45	Rear suspension coilover tab	30
46	Steering arm	31
47	Rear suspension clevis	31
48	Tie rod	32
49	Lower control arm clevis	32

List of Tables

1	Table of major vehicle dimensions	3
2	Summary of FEA results for suspension and steering components	14
3	Important Vehicle Parameters	18
4	Summary of worst case loading conditions	21

1 History

Midnight Sun was founded in 1988 at the University of Waterloo. The team has produced 11 solar-powered vehicles since its inception, numbered MSI through MSXI. MSX and its predecessors have been traditional Challenger class cars. MSXI was the team's first attempt at a Cruiser class vehicle, which ultimately suffered from design issues relating to its monocoque design. With MSXII, the team has regrouped and designed a new Cruiser vehicle from the ground up, focussing strongly on reliability, safety, and manufacturability.

2 Contacts

Questions regarding the design and implementation of MSXII should be directed to one of the following contacts:

Name	Title	Phone	Email
Tak Alguire	Project Manager	519-574-4610	tak.alguire@uwmidsun.com
Minghao Ji	Engineering Manager	519-500-1292	minghao.ji@uwmidsun.com
Devon Copeland	Mechanical Lead	226-792-7383	devon.copeland@uwmidsun.com
Titus Chow	Electrical Lead	226-978-7104	titus.chow@uwmidsun.com

3 Mechanical

3.1 Overview

MSXII is a dual-occupant Cruiser class vehicle. Its structural design uses a steel alloy tube chassis with non-structural fibreglass body panels. The majority of the vehicle's powertrain systems are located behind the occupant cell, including the battery pack, power junction box, motor controllers, and EV charger. The vehicle is rear-wheel driven by two hub-mounted DC motors. The locations of these components are marked in Figure 1 and Figure 2. Major vehicle dimensions are summarized in Table 1.

3.2 Chassis

3.2.1 Design

The chassis is a tube structure enclosing the occupant cell with small front and rear subframes to support suspension hardpoints. Smaller non-structural tube members will extend from the main frame to provide support to body panels as necessary. The majority of tubes are round, with square tubes being used only for elements intended to mount suspension and powertrain components (battery pack, motor controllers). Chassis elements use SAE 4130N chromoly tubes with diameters or side lengths ranging from 0.750" to 1.250", and wall thicknesses ranging from 0.035" to 0.065". Isometric drawings of the chassis are shown in Figures 3, 4, and 5.

3.2.2 Manufacturing

Bending, cutting, and profiling of tubes was done by an external supplier. Welding of the chassis was done by a professional welder using GTAW, with support from team members for jigging and assembly. A complete welding jig was designed in CAD and manufactured using 80/20 aluminum extrusion tubing, shown in Figure 6. Custom tube clamps were machined by the team to slot into jig members and fully support all chassis elements through multiple stages of assembly and welding.

3.2.3 Roll cage

The roll cage is integrated into the design of the chassis members enclosing the occupant cell. For the purposes of ASC regulations, the roll cage can be considered to include the A and B pillar hoops and elements connecting these two hoops lengthwise through the car. For clarity, these elements have been highlighted in Figure 7.

Wheelbase	2.60 m
Track	1.60 m
Max length	4.68 m
Max width	2.02 m
Max height	1.23 m

Table 1: Table of major vehicle dimensions

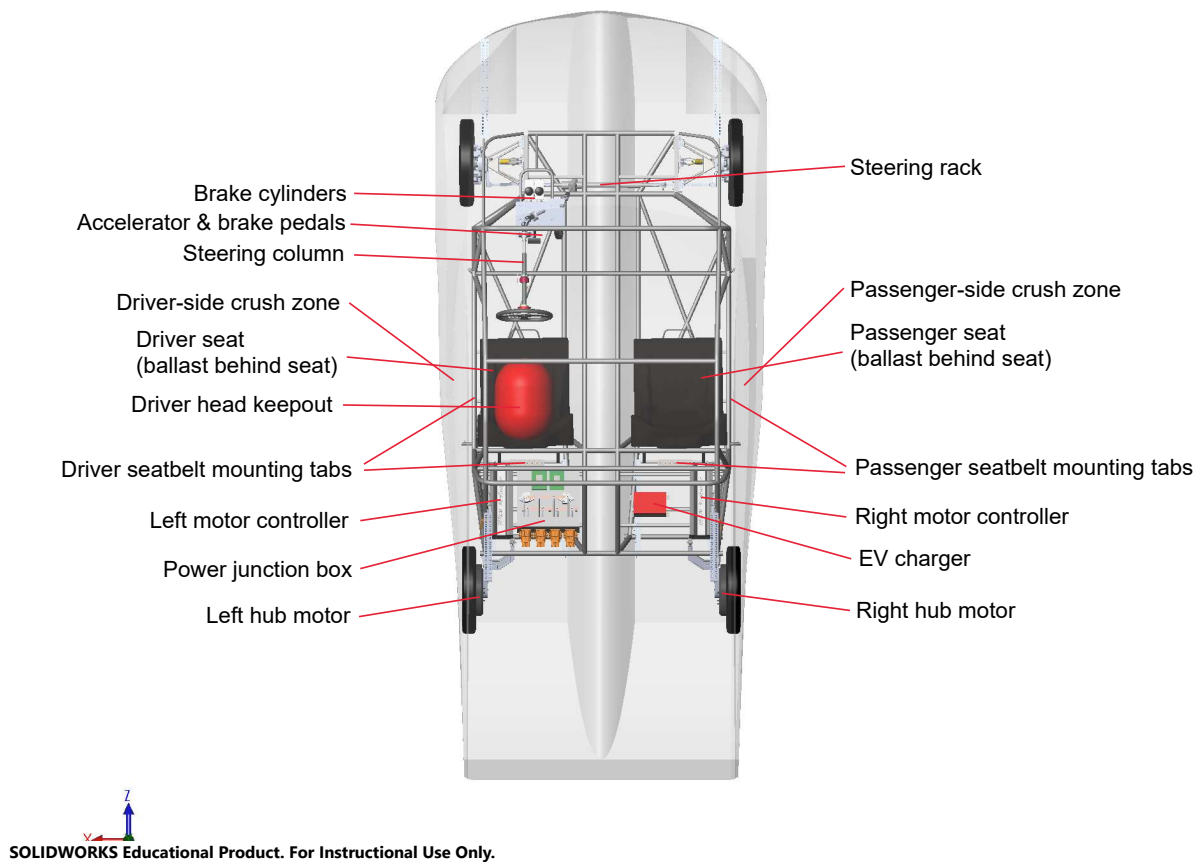
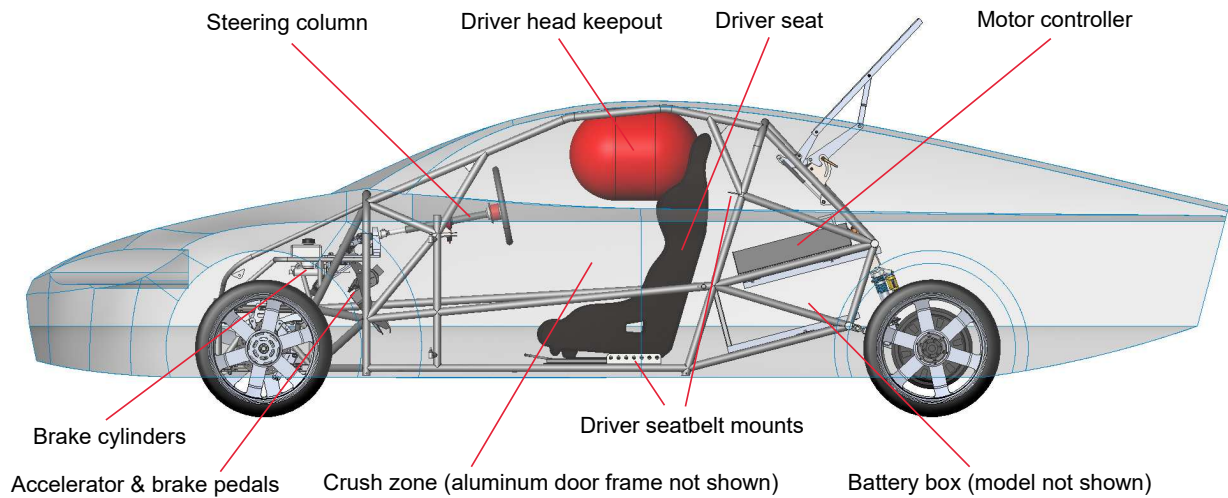


Figure 1: Top view showing major dimensions and system positions



SOLIDWORKS Educational Product. For Instructional Use Only.

Figure 2: Side view showing major dimensions and system positions

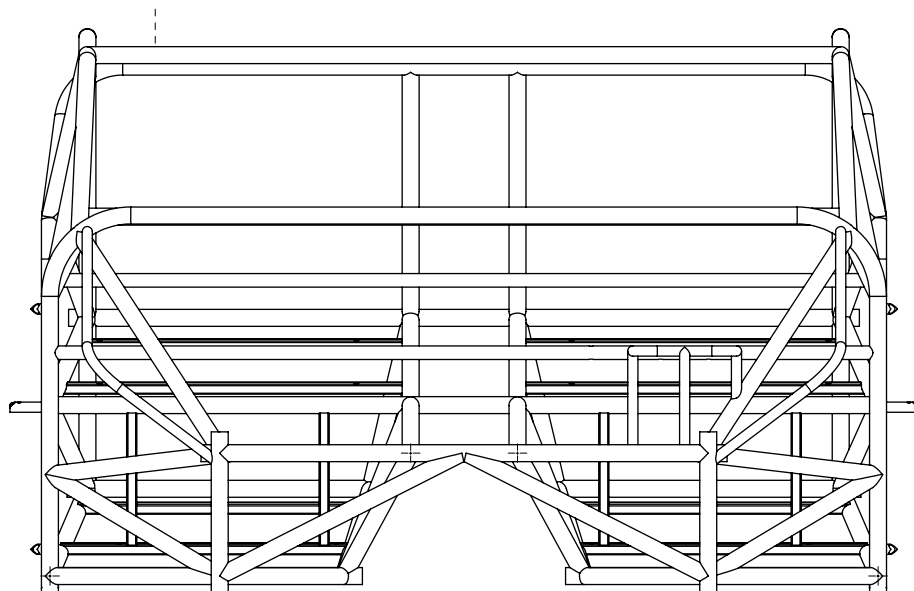


Figure 3: Chassis, front view

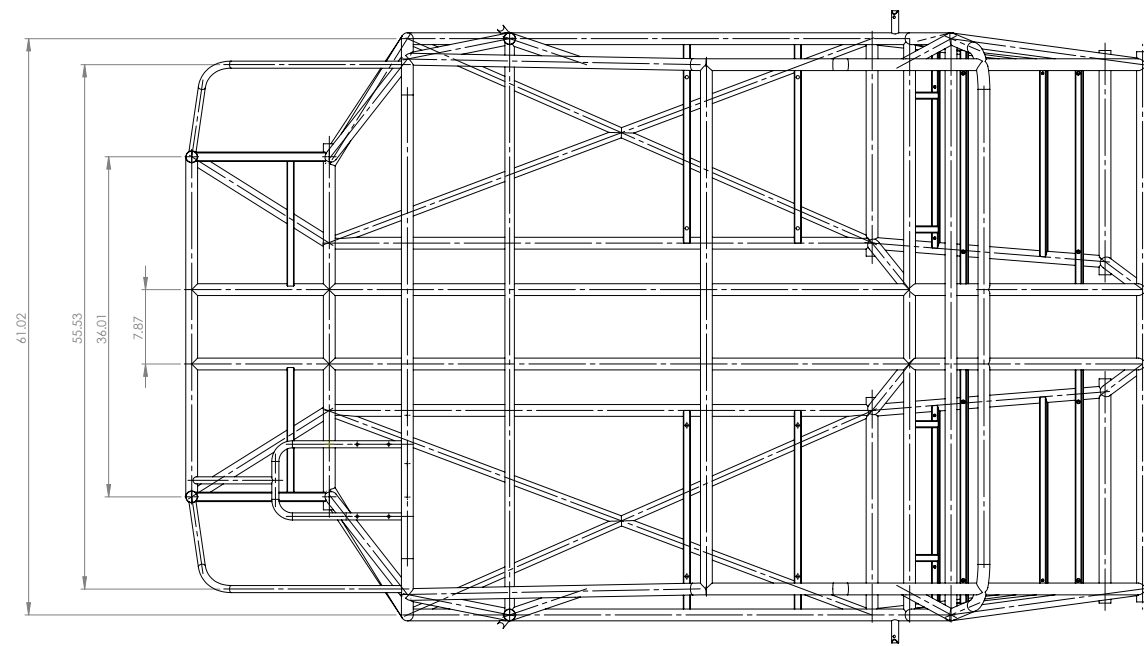


Figure 4: Chassis, top view

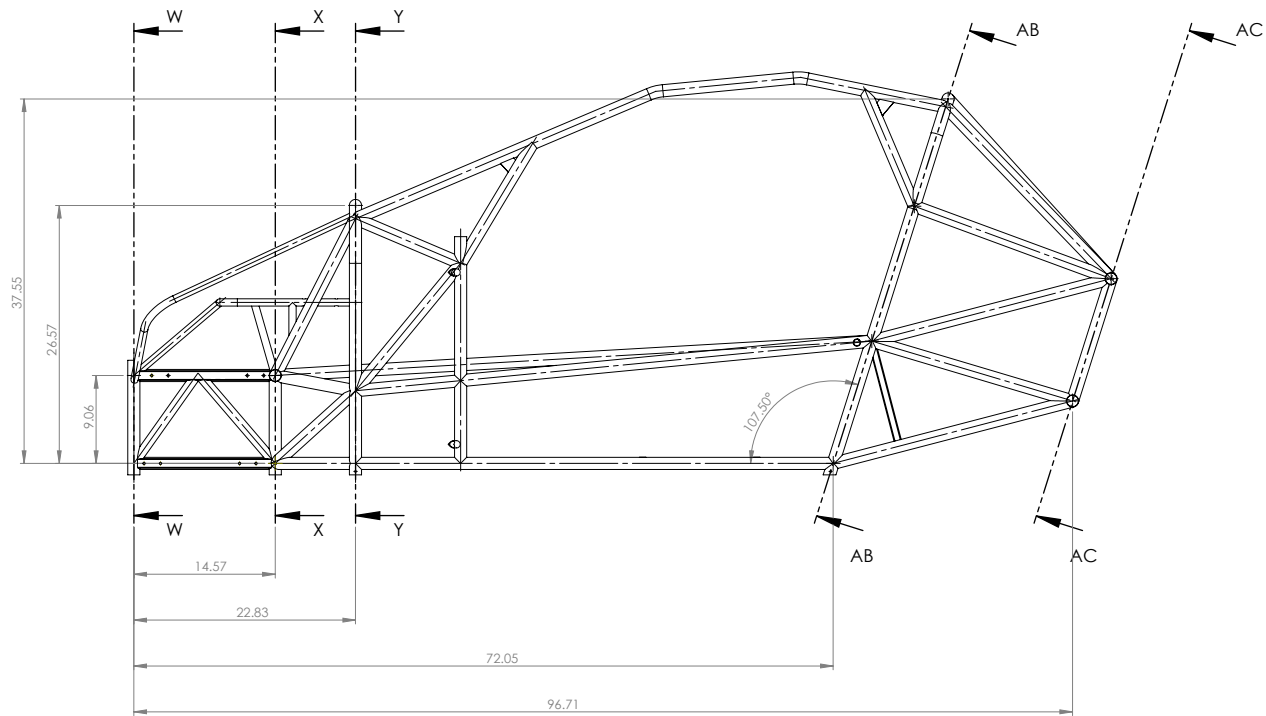
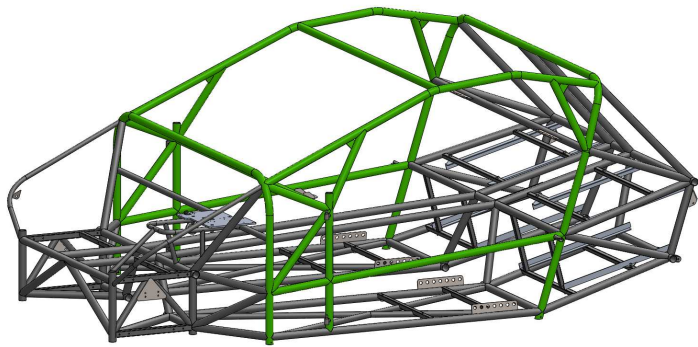


Figure 5: Chassis, side view



Figure 6: Welding jig on rotating mount



SOLIDWORKS Educational Product. For Instructional Use Only.

Figure 7: Chassis with roll cage elements highlighted

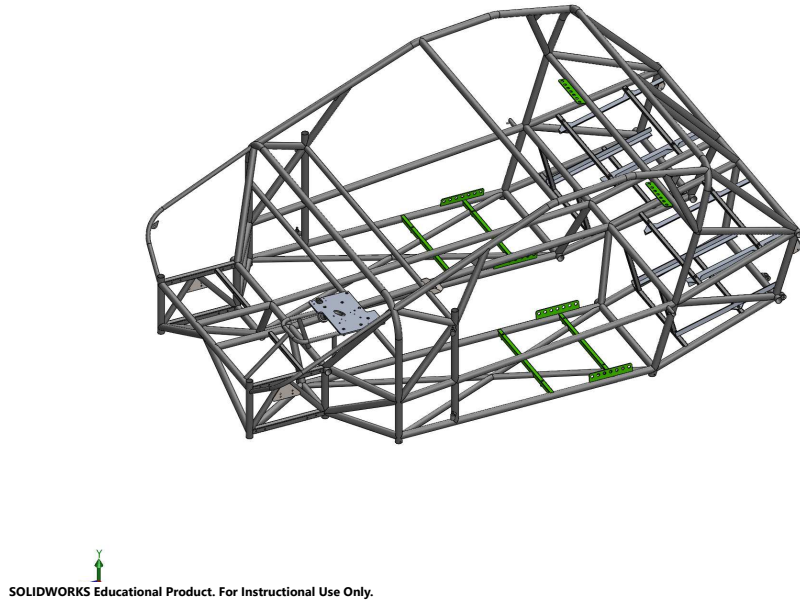


Figure 8: Chassis mounting points for seat belts

3.3 Seat belts

MSXII is equipped with 5-point seat belts for both occupants. Seat belt hardpoints are mounted to metal tabs welded to chassis members, shown in Figure 8. Figure 9 shows one of these tabs. Figures 10 and 11 demonstrate compliance with ASC regulations 10.3.E.

3.4 Braking system

3.4.1 Primary brakes

The primary braking system is designed with dual redundant front braking, consisting of two identical systems with separate master cylinders, hydraulic lines, and calipers to each of the left and right wheels. The master cylinders are operated in unison via a single mechanical brake pedal. A schematic of the primary system is shown in Figure 12.

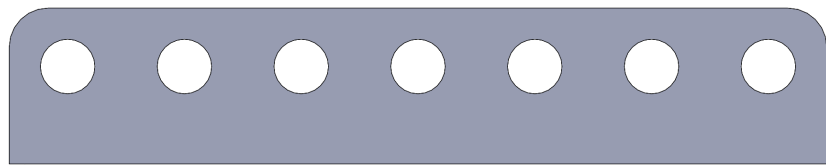
Front brake calipers are Willwood parts 120-8374 (left) and 120-8373 (right). Willwood's website indicates the caliper pads have 2 in^2 (12.9 cm^2) contact area and 0.30" (7.6 mm) depth including the backing plate.

The master cylinders are Willwood part 206-3374. They have a 3/8"-24 outlet size which will need to be connected via a suitable brake line to the M10 x 1.25 inlets of the calipers. Brake lines will be DOT-approved hose assemblies sized for 3/8"-24 on one end and M10 on the other end via a banjo joint. The brake pedal is Willwood part 340-15079 and is mounted in the standard configuration to the left of the accelerator pedal.

Brake rotors will be custom-machined to the disk thickness and diameter supported by the Willwood calipers. All mounting geometry on the suspension upright for primary calipers are designed to position the primary calipers in the optimal positions to meet braking specifications.

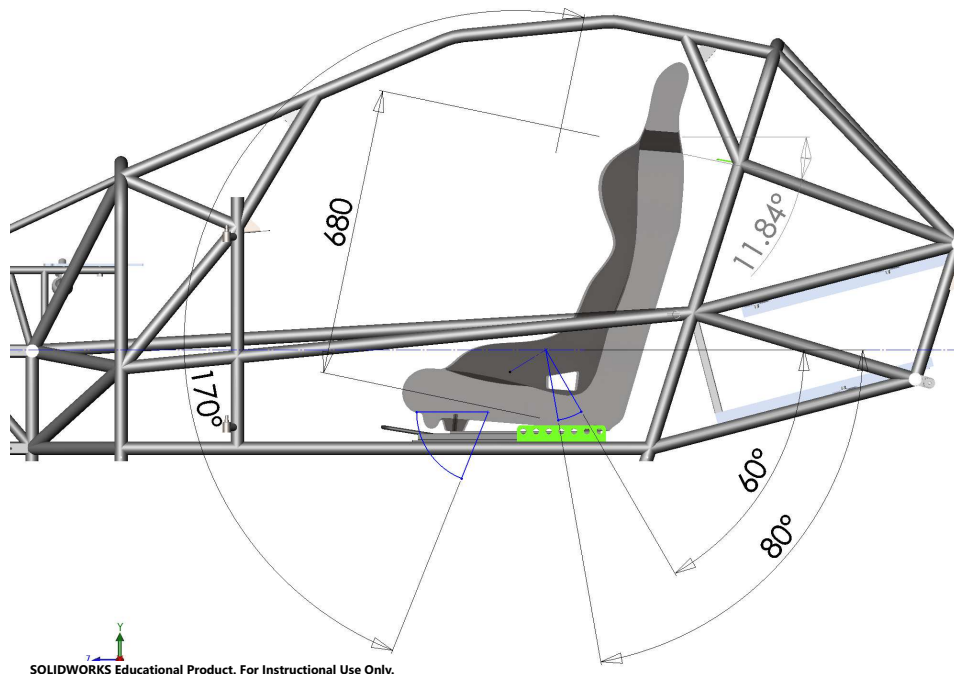
3.4.2 Parking brake

The parking brake will be implemented by a cable-actuated caliper mounted at one of the front wheels. The caliper is the Tolomatic ME10LA, part number 0732-0003. It will share the same brake disk as the primary braking system but is otherwise mechanically independent. Due to unresolvable dimensioning differences between



SOLIDWORKS Educational Product. For Instructional Use Only.

Figure 9: Single seat belt tab



SOLIDWORKS Educational Product. For Instructional Use Only.

Figure 10: Side view of seat belt geometry

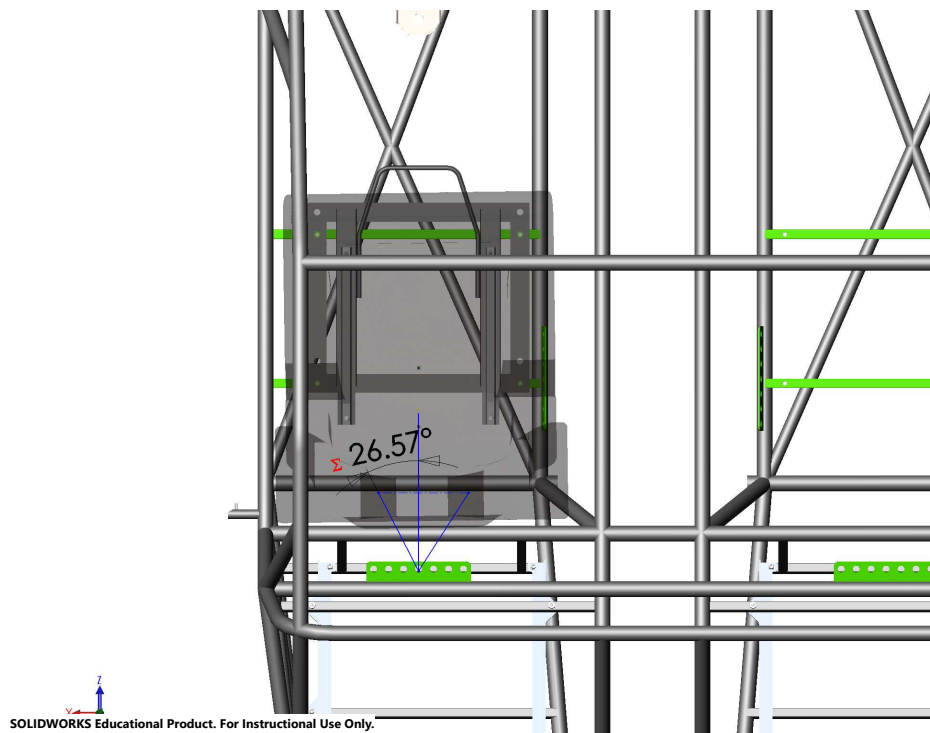


Figure 11: Top view of seat belt geometry

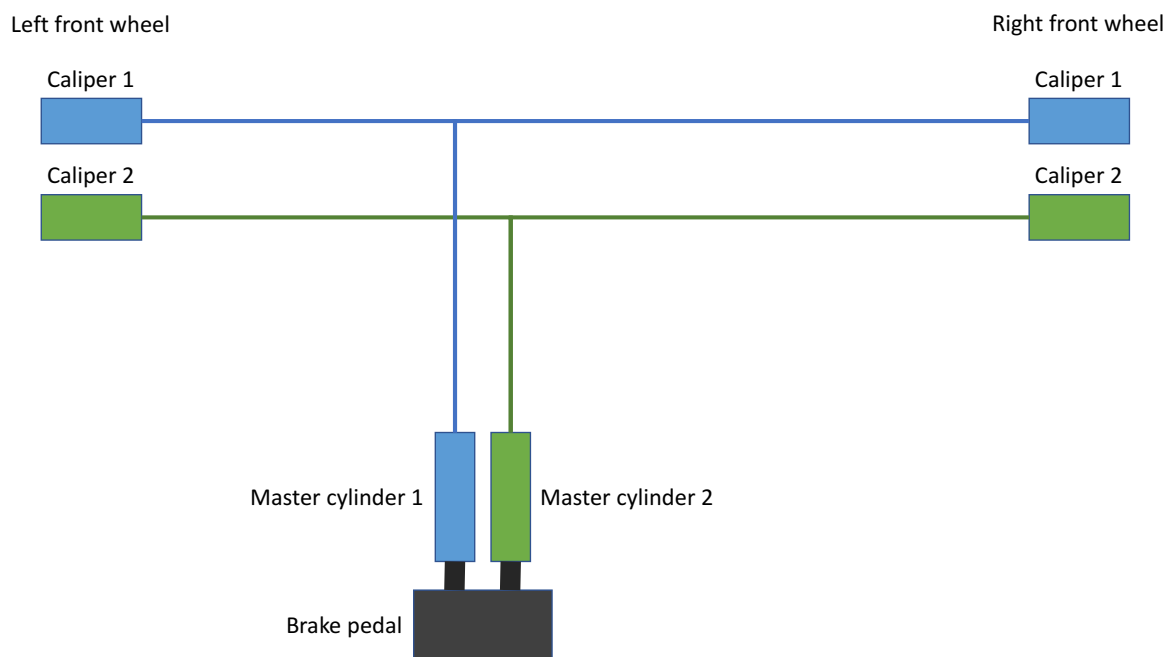


Figure 12: Schematic of primary braking system

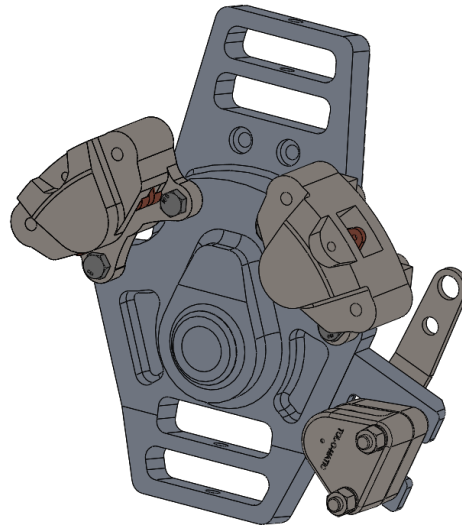


Figure 13: View of dual-primary calipers and parking caliper on front suspension upright

the Tolomatic and Willwood calipers, the parking brake caliper cannot be mounted perfectly as per the manufacturer's recommendations and will have only 80% overlap with the brake disk. However, this is expected to provide more than sufficient countertorque to keep the vehicle stationary as per ASC regulations 10.6.

Figure 13 shows a front suspension upright with all three calipers mounted (two primary and one parking).

3.5 Steering system

The steering system uses a rear-steering, left-hand-drive rack and pinion from Helix (part number 188754). The system uses a collapsible steering column from Sweet Mfg., part number 405-10310. The linkage uses dual U-joints to circumvent interfering brake system components and is shown in Figure 14.

3.6 Suspension

3.6.1 Front suspension

The front suspension uses dual A-arms with an outboard damper and coilover spring. The upper and lower control arms are custom-built from 4130 chromoly tubes. The damper and coilover are a single integrated assembly supplied by Öhlins, sold as the TTX25, which is marketed for Formula SAE vehicles. Figure 15 shows the front suspension assembly.

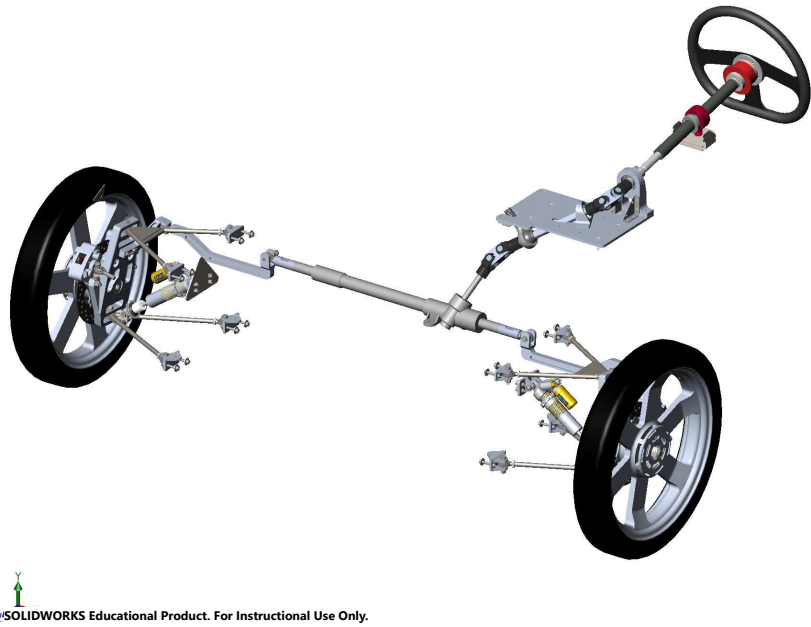
The front suspension lower control arm bears the majority of the shear stress from road forces. Based on hand calculations for a cantilever beam, the worst-case von Mises stress is 183 MPa. This dictates the sizing of the rod end.

3.6.2 Rear suspension

The rear suspension uses independent trailing arms mounted outwards from the rear of the chassis. The trailing arm itself is custom-machined and mounts the same Öhlins TTX25 shock absorber as the front suspension. Figure 16 shows the rear suspension assembly.

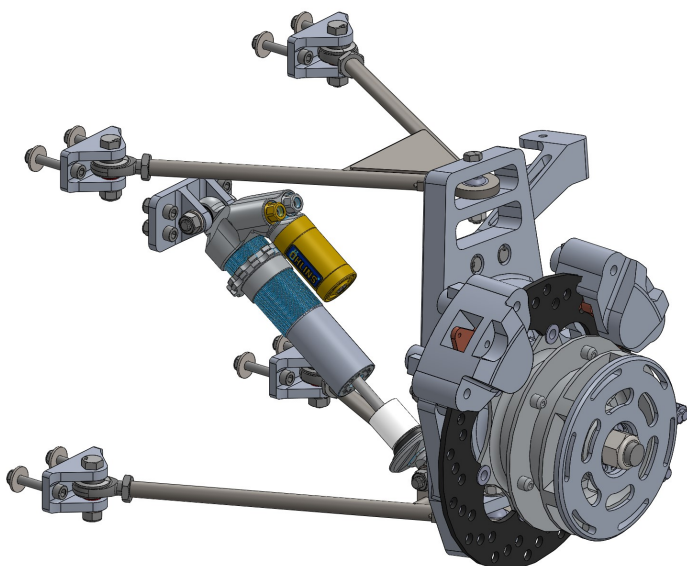
3.7 Finite element analysis

Finite element analysis was performed using ANSYS on the chassis and all suspension and steering components (downstream from the rack and pinion). FEA of the chassis followed the specifications provided by the ASC



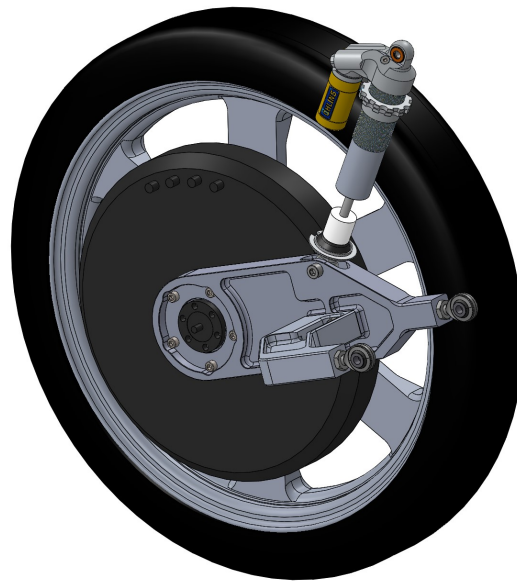
 SOLIDWORKS Educational Product. For Instructional Use Only.

Figure 14: View of steering assembly



 SOLIDWORKS Educational Product. For Instructional Use Only.

Figure 15: View of front suspension assembly (parking brake caliper obstructed by hub)



SOLIDWORKS Educational Product. For Instructional Use Only.

Figure 16: View of rear suspension assembly

regulations. A general methodology was to fix a solid beam or wall in space, and apply a 5G acceleration to the chassis against it. Images for FEA simulations of each requested scenario are shown in Appendix B.

Worst-case loading forces on each wheel were used to derive appropriate constraints and forces for FEA simulation of the suspension and steering system. A complete derivation and summary of loading forces on each wheel is given in Appendix A. Images of all FEA simulations for suspension and steering are available in Appendix C.

3.7.1 Front suspension

Clevises Hand calculations were used to resolve the forces from the road as loading onto the clevises. The back face of the clevis was constrained with compression only support. Cylindrical supports were used for the bolt holes and fasterner pretension was added. Frictional contacts were added between the fasteners and the clevis.

Control arms Contacts were modeled between the control arm tubes and the bearing plate. Forces were applied to the bearing plate based on hand calculations.

Uprights A dummy wheel was modeled to which forces were applied. The dummy wheel contacted the spindle with a frictional contact which when applied a load to the upright. The brake forces were applied to the caliper mounting holes. Assuming only one break caliper were taking all the force.

Spindle A dummy wheel was modeled to which forces were applied. The dummy wheel contacted the spindle with a frictional contact which when applied a load to the upright.

Upper bearing plate Contacts were modeled between the control arm tubes and the bearing plate, forces were applied to the bearing plate based on hand calculations.

Part Number	Part Name	Material	Max Stress (MPa)	Safety Factor
MS00015	Coilover Clevis	Aluminum, 7075	147	3.4
MS00029	Upper Control Arm Clevis	Aluminum, 7075	191	2.6
MS00102	Lower Control Arm Clevis	Aluminum, 7075	198	2.5
MS00017	Upper Control Arm	Chromoly Steel, 4130	199	2.3
MS00018	Lower Control Arm	Chromoly Steel, 4130	X	X
MS00019	Upright	Aluminum, 7075	210	2.4
MS00020	Spindle	Chromoly Steel, 4140	177	2.3
MS00030	Upper Bearing Plate	Chromoly Steel, 4130	141	3.3
MS00036	Coilover Control Arm Tab	Chromoly Steel, 4130	159	2.9
MS00038	Coilover Mounting Plate	Chromoly Steel, 4130	147	3.1
MS00086	Rear Suspension Clevis Mount	Chromoly Steel, 4130	231	2.0
MS00047	Rear Suspension Coilover Tab	Chromoly Steel, 4130	147	3.1
MS00025	Trailing Arm	Aluminum, 7075	X	X
MS00026	Rear Brace	Aluminum, 7075	X	X
MS00074	Steering Arm	Aluminum, 6061-T6	77	3.5
MS00101	Tie Rod	Aluminum, 6061-T6	41	6.6

Table 2: Summary of FEA results for suspension and steering components

Coilover control arm tab The maximum force on the front wheel was resolved as a compressive load in the coilover and applied to this tab.

Coilover mounting plate Hand calculations were used to resolve the forces from the road as loading onto the clevises. For this simulation a frictional contact was added between the clevis and the mounting plate. Dummy chassis tubes were modeled behind the mounting plate and welded edges were fixted.

3.7.2 Rear suspension

Clevises The worst case of four loading scenarios was taken (2 clevis positions, each with either inside or outside wheel when rounding a corner). It was assumed that all the lateral force was applied to a single clevis because this is a statically indeterminate problem on paper (so went with worst case).

Coilover tab The maximum normal force and acceleration force on the rear wheel was resolved as a compressive load in the coilover and applied to this tab.

3.7.3 Steering

Steering arms A compression support was added on the face datuming off of the upright. The maximum lateral force on the tire during 1G cornering was resolved as a torque on the upright. This torque was applied by a bearing load acting at the end of the steering arm.

Tie rods A similar analysis to that for the steering arm was used. Force was applied to one end of the tie rod while the other remained fixed. Both sides of the tie rod were tested with an applied force and fixed support.

3.7.4 Results

All FEA results for suspension and steering components are summarized in Table 2. Note that FEA for the rear suspension trailing arm and brace, as well as front suspension lower control arm, are currently unavailable. Simulations of the rear trailing arm are experiencing convergence and stress concentration issues. The front lower control arm is undergoing slight modifications to increase its safety factor under maximum loading conditions.

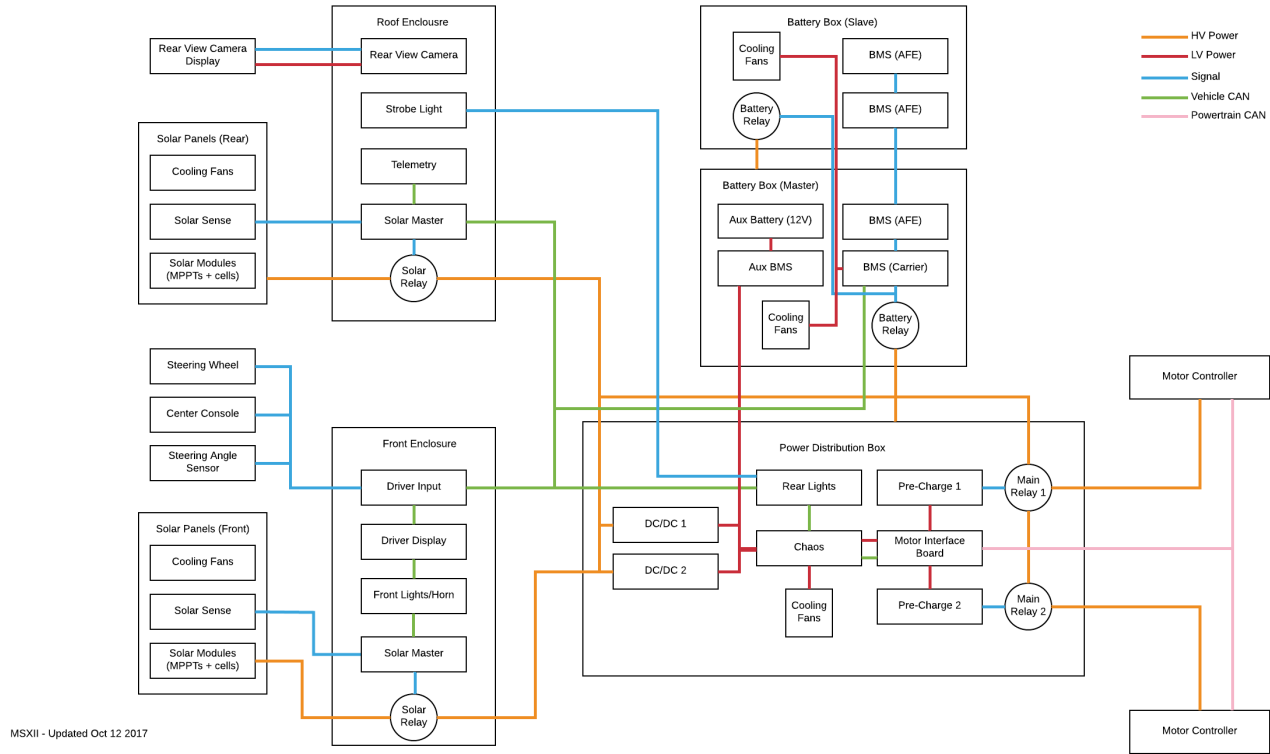


Figure 17: Block diagram of all electrical systems

4 Electrical

4.1 Overview

Midnight Sun XII's electrical system consists of high- and low-voltage domains that are electrically isolated for safety. The high-voltage system includes the Sunpower E-series solar cells, Nomura maximum power point trackers, Tritium motor controllers and NGM SCM-150 motors. These are externally-sourced components purchased by the team and interface with the vehicle's custom embedded systems.

The low-voltage system is comprised of custom circuit-boards serving several functions for monitoring and controlling the vehicle, primarily: driver controls, power distribution, battery management, and external lights. Several smaller PCBs are located throughout the vehicle to support various sensor interfacing and data collection functions. Most boards communicate over a unified CAN bus, with some nodes supporting smaller subsystems over I²C or SPI. The low-voltage power rail is normally provided by the main battery pack via DC-DC converters, but can also be switched to an auxiliary 12V Ni-MH battery during startup or fault modes.

Due to the different CAN specifications of the Tritium WaveSculptor motor controllers, they are allocated a separate powertrain CAN network which interfaces with the primary CAN bus via dedicated transceiver boards. A block diagram of all electrical systems is shown in Figure 17. A block diagram of only the vehicle's high-voltage systems is shown in Figure 18.

4.2 Battery

For MSXII the team chose to use MJ1 18650 cells produced by LG Chem Ltd. 36 MJ1 cells are put in parallel to form a module, and 36 modules are put in series to provide a 130.86 V nominal, 16.5 kWh capacity battery pack. Within each module, cells will be spot welded to nickel tabs, which are themselves soldered to copper bus bars forming a high-ampacity interconnect. Bus bars of adjacent modules are mechanically connected together to create series connections through the pack.

The cells were sourced from Liion Wholesale in early 2017.

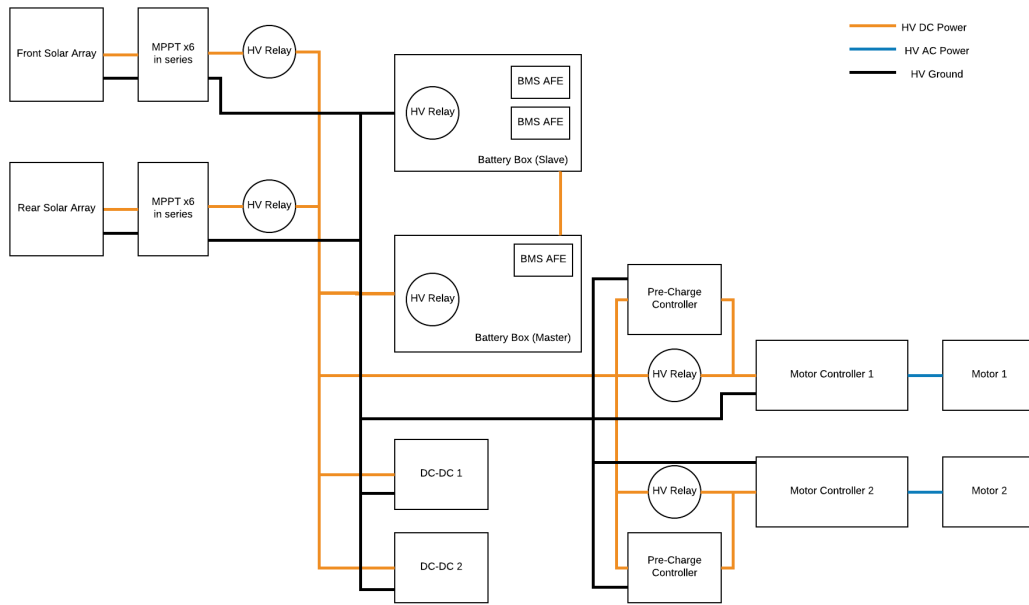


Figure 18: Block diagram of all high-voltage electrical systems

4.2.1 Testing Methodology

Battery testing is expected to be completed in 4 main phases, outlined below.

Phase One The first phase requires verification of the battery management system (BMS). This will test the system's ability to measure and monitor voltage, current, and temperature measurements from each of the modules. The system must be able to correctly respond to under-voltage, over-voltage, over-current, and over-temperature conditions to demonstrate that the BMS can actively protect the battery. Phase one is currently underway and is expected to be complete by November 2017.

Phase Two The second phase requires testing module performance and reliability. A prototype module containing 36 cells in parallel will be built and tested. This module will undergo charge cycle tests using a benchtop power supply and an electronic load. The BMS will be connected to log data and ensure safety. The team will then build 3 battery modules to test the series connections between modules. Phase two is expected to be complete by December 2017.

Phase Three The third phase involves the full manufacturing and testing of the battery pack. The team will be able to assess the overall performance of the battery and make necessary modifications to the cooling system prior to installing the battery in the car. The pack will be discharged at 1C, which is approximately 120A of current. This will be accomplished by either powering the vehicle motors mounted to a dynamometer, or by using a salt water load with a resistance designed for the target current draw. Phase three is expected to be completed by the end of January 2018.

Phase Four The final phase of battery testing will involve building a mechanical enclosure and integrating the pack into the vehicle. With a drivable vehicle, the team will be able to test the pack under real world conditions, and make any changes necessary prior to the race. Reliability of the modules and connections under harsh

environmental conditions can be evaluated during road tests. Since this requires the vehicle to be in a drivable state, it is expected to begin in April or May 2018 and finish before July.

Mass (M)	550	kg
Wheelbase	2.60	m
Track	1.60	m
Tire Diameter	0.53	m
Wheel Assembly Moment of Inertia (J_w)	0.25	kg m^2
Distance from Front Wheel to CoG (a)	1.32	m
Distance from Front Wheel to CoG (b)	1.28	m
Distance from Road to CoG (h)	0.52	m
Full Wheel Travel in Compression	45	mm
Front Coilover Angle from Vertical	40	°
Rear Coilover Angle from Vertical	30	°

Table 3: Important Vehicle Parameters

A Loading conditions

FEA of the chassis, suspension, and steering system was done using ANSYS software. Loading conditions were derived from both ASC requirements and real-world scenarios. Assuming a smooth driving surface, the largest normal force acting on the front tire will occur while braking in a turn. Similarly, the largest normal force acting on the rear tire will occur while accelerating in a turn. To approximate these loading condition, the a superposition of two static half car models is used; one for cornering and one for hard braking.

Table 3 lists vehicle parameters that are relevant in determining the loading conditions in the suspension. The mass and moment of inertia were computed using CAD software.

A.1 Braking

Figure 19 shows a free body diagram of a half car model undergoing braking. The required braking force can be approximated as follows:

$$F_{\text{braking}} = F_{\text{Nf}} + F_{\text{Nr}} = Mg = (550 \text{ kg})(9.81 \text{ m s}^{-2}) = 5.40 \text{ kN} \quad (1)$$

From Figure 19, summing the moments about the centre of gravity and the vertical forces results in the following equations:

$$aF_{\text{Nf}} = hF_{\text{braking}} + bF_{\text{Nr}} \quad (2)$$

$$F_{\text{Nf}} + F_{\text{Nr}} = Mg \quad (3)$$

Solving for the front normal force:

$$\begin{aligned} aF_{\text{Nf}} &= hF_{\text{braking}} + b(Mg - F_{\text{Nf}}) \\ F_{\text{Nf}} &= \frac{hF_{\text{braking}} + bMg}{a + b} = \frac{(0.52 \text{ m})(5.40 \text{ kN}) + (1.28 \text{ m})(550 \text{ kg})(9.81 \text{ m s}^{-2})}{(1.32 \text{ m}) + (1.28 \text{ m})} = 3.74 \text{ kN} \end{aligned} \quad (4)$$

Note that 3.74 kN is for both front wheels. Therefore there is approximately 1.87 kN of normal force on each front tire during hard braking.

A.2 Acceleration

MSXII uses NGM SCM-150 motors which have a peak torque of 135 N m. From this torque value and a number of other vehicle parameters the vehicle's maximum acceleration can be calculated as follows:

$$a = \frac{F_w}{\frac{1}{2}M} \quad (5)$$

$$\alpha_w = \frac{T_m - F_w r}{J_w} \quad (6)$$

$$\alpha_w = ar \quad (7)$$

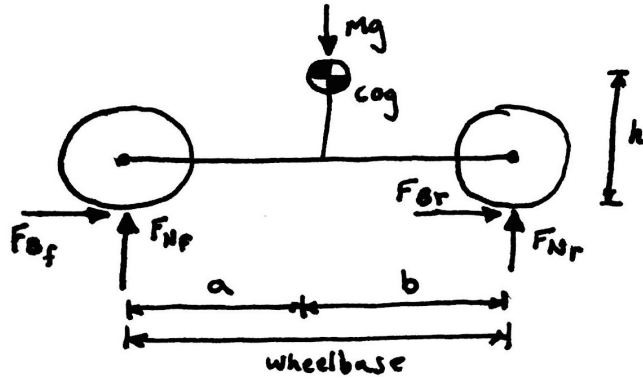


Figure 19: Free body diagram of vehicle braking

where a is the acceleration of the vehicle, F_w is the friction force acting on a single tire while accelerating, J_w is the moment of inertia of the wheel assembly, r is the radius of the tire, T_m is the torque from the motor and α_w is the angular acceleration of the wheel.

Rearranging the above three equations, the acceleration of the vehicle can be expressed as a function of motor torque as follows:

$$a = \frac{T_m r}{\frac{1}{2} M r^2 + J_w}$$

$$a = \frac{(135 \text{ N m})(0.27 \text{ m})}{\frac{1}{2}(550 \text{ kg})(0.27 \text{ m}^2)^2 + 0.25 \text{ kg m}^2} = 1.80 \text{ m s}^{-2} \quad (8)$$

Solving for friction force on a single rear tire:

$$F_w = Ma = (550 \text{ kg})(1.80 \text{ m s}^{-2}) = 990 \text{ N} \quad (9)$$

The resulting normal force on the rear wheels can be calculated as follows:

$$bF_{Nr} = hF_w + a(Mg - F_{Nr})$$

$$F_{Nr} = \frac{hF_w + aMg}{a + b} = \frac{(0.52 \text{ m})(990 \text{ N}) + (1.32 \text{ m})(550 \text{ kg})(9.81 \text{ m s}^{-2})}{(1.32 \text{ m}) + (1.28 \text{ m})} = 2.94 \text{ kN} \quad (10)$$

Note that 2.94 kN is for both rear wheels. Therefore there is approximately 1.47 kN of normal force on each rear tire during maximum acceleration.

A.3 Cornering

ASC regulations require simulations of a 1G turn, at minimum. This corresponds to the following lateral force:

$$F_{steer} = Mg = (550 \text{ kg})(9.81 \text{ m s}^{-2}) = 5.40 \text{ kN} \quad (11)$$

Additionally, the diameter of several highway exit ramps around the University of Waterloo were measured on satellite maps. The recommended speed limit on these exits is 50 km h^{-1} . Assuming a worst case scenario where the vehicle takes an exit with a 100 m diameter at 80 km h^{-1} (22.22 m s^{-1}), the required lateral force required to navigate this corner can be found as follows:

$$F_{steer} = \frac{Mv^2}{r} = \frac{(550 \text{ kg})(22.22 \text{ m s}^{-1})^2}{50 \text{ m}} = 5.43 \text{ kN} \quad (12)$$

This corresponds nearly identically to a 1G turn. Since the lateral force required in the second scenario is slightly higher, 5.34 kN will be used as the worst case cornering force.

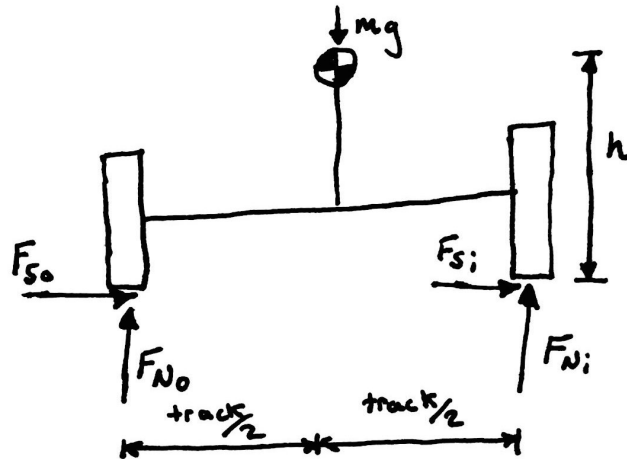


Figure 20: Free Body Diagram of a Car Cornering

Using the half car model shown in Figure 20, summing the moments about the centre of gravity and the vertical forces results in the following equations:

$$\frac{1}{2}L_{\text{track}}F_{No} = hF_{steer} + \frac{1}{2}L_{\text{track}}F_{Ni} \quad (13)$$

$$F_{No} + F_{Ni} = Mg \quad (14)$$

Solving for the outside wheel normal force:

$$\begin{aligned} \frac{1}{2}L_{\text{track}}F_{No} &= hF_{steer} + \frac{1}{2}L_{\text{track}}(Mg - F_{Ni}) \\ F_{No} &= \frac{hF_{steer} + \frac{1}{2}L_{\text{track}}Mg}{L_{\text{track}}} = \frac{(0.52 \text{ m})(5.43 \text{ kN}) + (0.80 \text{ m})(550 \text{ kg})(9.81 \text{ m s}^{-2})}{1.60 \text{ m}} = 4.46 \text{ kN} \end{aligned} \quad (15)$$

Solving for the inside wheel normal force:

$$F_{Ni} = Mg - F_{No} = (550 \text{ kg})(9.81 \text{ m s}^{-2}) - 4.46 \text{ kN} = 0.93 \text{ kN} \quad (16)$$

Note that the forces above are for both front and rear outside wheels. Assuming the force is evenly split between the front and rear, there is approximately 2.23 kN of normal force on each outside tire and 0.47 kN for each inside tire during maximum cornering.

A.4 Bump

As stipulated in the ASC 2018 regulations, the analysis for suspension and steering must include loading considerations for a 2G bump. We interpret this requirement as the body of the vehicle accelerating upwards at 2G, in which case the additional normal force subjected to a single tire can be expressed as follows:

$$F_{N,\text{bump}} = \frac{2Mg}{4} = \frac{2(9.81 \text{ m s}^{-2})(550 \text{ kg})}{4} = 2.70 \text{ kN} \quad (17)$$

A.5 Superposition

The braking, accelerating, and cornering conditions subject the wheels to normal forces that differ from those experienced when the car is at rest. The change in normal force for each loading condition can be expressed

as follows:

$$\Delta F_{Nf,\text{braking}} = F_{Nf,\text{braking}} - \frac{Mg}{4} = 1.87 \text{ kN} - 1.35 \text{ kN} = 0.52 \text{ kN} \quad (18)$$

$$\Delta F_{Nr,\text{accelerating}} = F_{Nr,\text{accelerating}} - \frac{Mg}{4} = 1.47 \text{ kN} - 1.35 \text{ kN} = 0.12 \text{ kN} \quad (19)$$

$$\Delta F_{No,\text{cornering}} = F_{No,\text{cornering}} - \frac{Mg}{4} = 2.23 \text{ kN} - 1.35 \text{ kN} = 0.88 \text{ kN} \quad (20)$$

$$\Delta F_{Ni,\text{cornering}} = F_{Ni,\text{cornering}} - \frac{Mg}{4} = 0.47 \text{ kN} - 1.35 \text{ kN} = -0.88 \text{ kN} \quad (21)$$

$$\Delta F_{N,\text{bump}} = F_{N,\text{bump}} - \frac{Mg}{4} = 2.70 \text{ kN} - 1.35 \text{ kN} = 1.35 \text{ kN} \quad (22)$$

To approximate the worst case loading condition, a superposition of the changes in normal force and the nominal normal force is applied. Note that the nominal force used is the same for each wheel, which assumes a centre of gravity approximately centred along the wheelbase.

$$F_{Nfi,\text{max}} = \Delta F_{Nf,\text{braking}} + \Delta F_{Ni,\text{cornering}} + 2F_{N,\text{nominal}} = 0.52 \text{ kN} - 0.88 \text{ kN} + 2.70 \text{ kN} = 2.34 \text{ kN} \quad (23)$$

$$F_{Nfo,\text{max}} = \Delta F_{Nr,\text{braking}} + \Delta F_{No,\text{cornering}} + 2F_{N,\text{nominal}} = 0.12 \text{ kN} - 0.88 \text{ kN} + 2.70 \text{ kN} = 4.10 \text{ kN} \quad (24)$$

$$F_{Nri,\text{max}} = \Delta F_{Nf,\text{braking}} + \Delta F_{Ni,\text{cornering}} + 2F_{N,\text{nominal}} = 0.52 \text{ kN} + 0.88 \text{ kN} + 2.70 \text{ kN} = 1.94 \text{ kN} \quad (25)$$

$$F_{Nro,\text{max}} = \Delta F_{Nr,\text{braking}} + \Delta F_{No,\text{cornering}} + 2F_{N,\text{nominal}} = 0.12 \text{ kN} + 0.88 \text{ kN} + 2.70 \text{ kN} = 3.70 \text{ kN} \quad (26)$$

A.6 Summary

Table 4 summarizes the loading conditions used for static structural FEA simulations on the suspension and steering components. Note that the direction of the force corresponds with the global coordinate system of the MSXII and the vectors shown in Figure 21. The assemblies shown are for the driver's side of the vehicle

Table 4: Summary of worst case loading conditions

Worst Case Loading	F_x (kN)	F_y (kN)	F_z (kN)
Braking & Cornering (Inside Front Wheel)	2.72	2.34	2.70
Braking & Cornering (Outside Front Wheel)	-2.72	4.10	2.70
Accelerating & Cornering (Inside Rear Wheel)	2.72	1.94	0.99
Accelerating & Cornering (Outside Rear Wheel)	-2.72	3.70	0.99

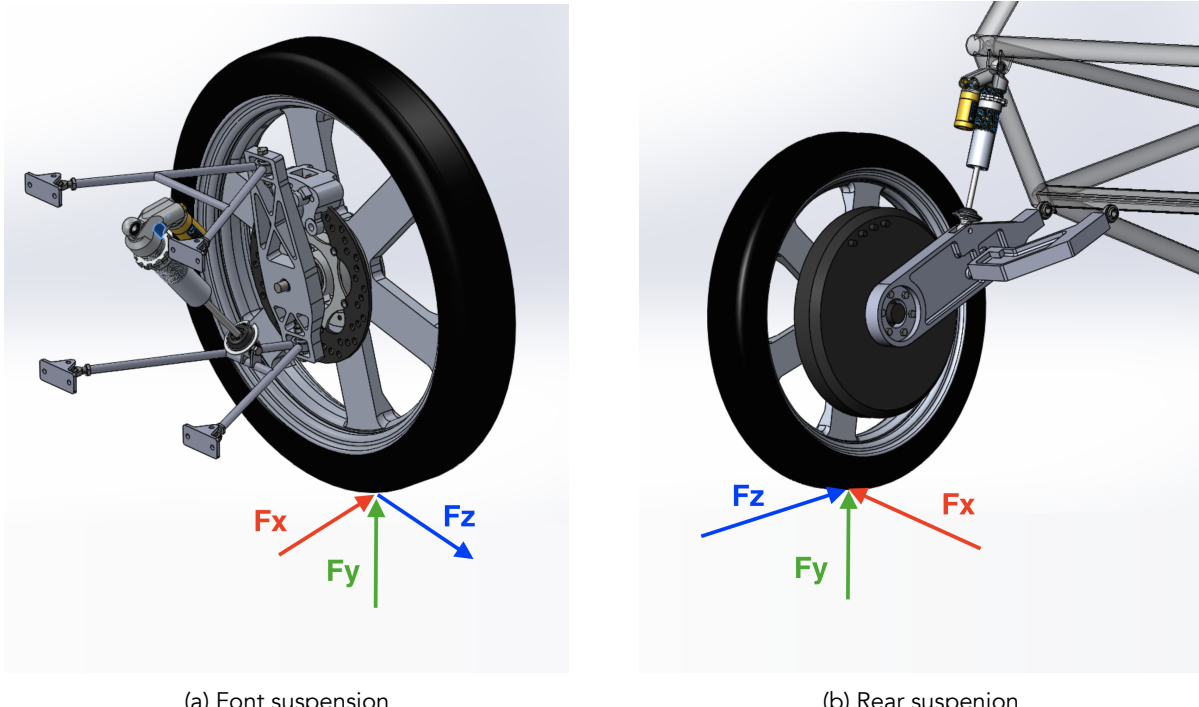


Figure 21: Suspension coordinate system

B FEA images for chassis

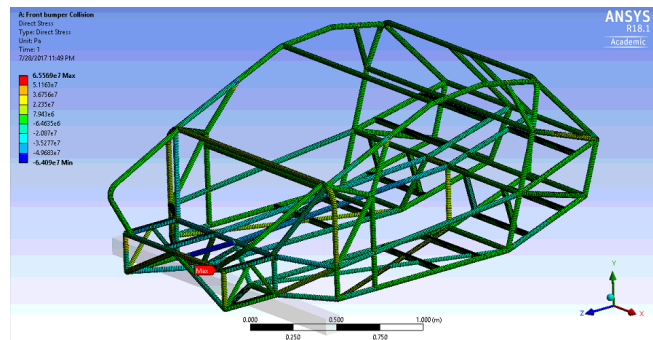


Figure 22: Front bumper collision

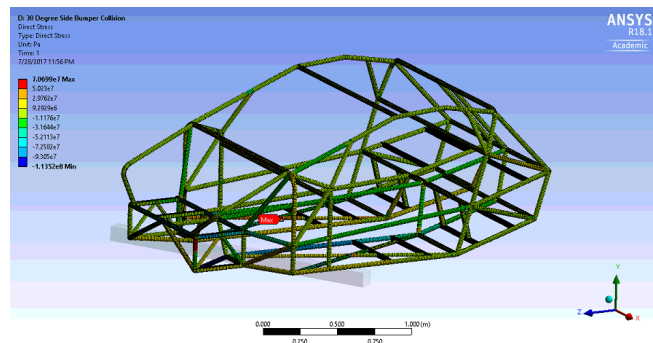


Figure 23: Front bumper 30 degree collision

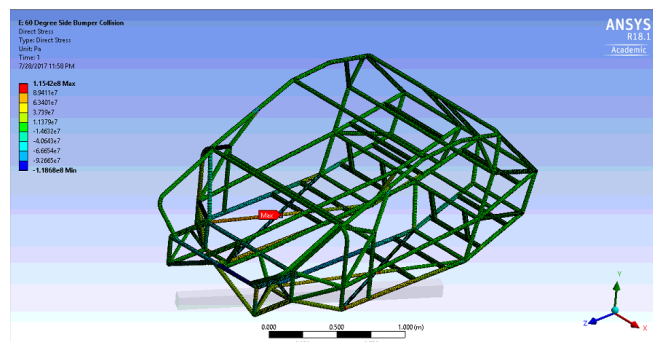


Figure 24: Front bumper 60 degree collision

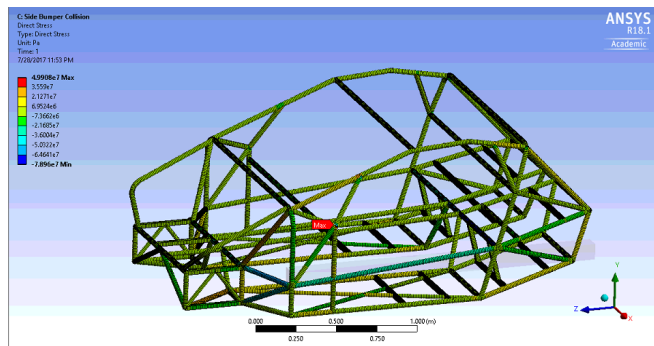


Figure 25: Side bumper collision

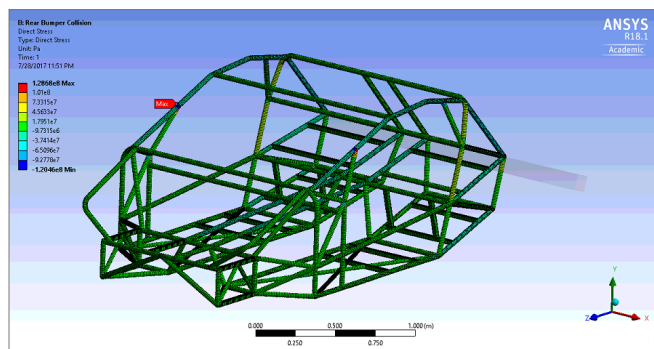


Figure 26: Rear bumper collision

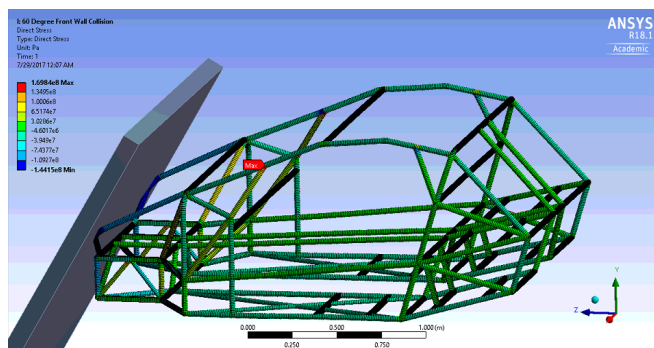


Figure 27: Hood 60 degree collision

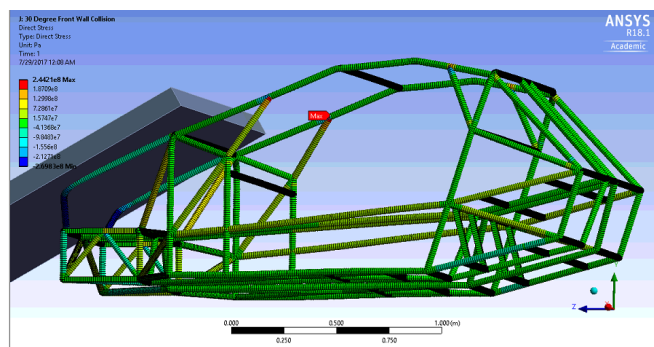


Figure 28: Hood 30 degree collision

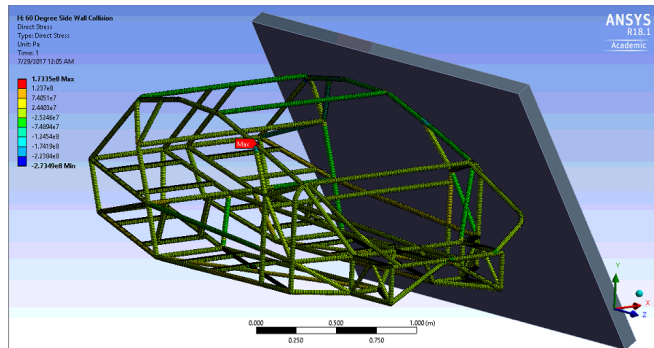


Figure 29: Side 60 degree collision

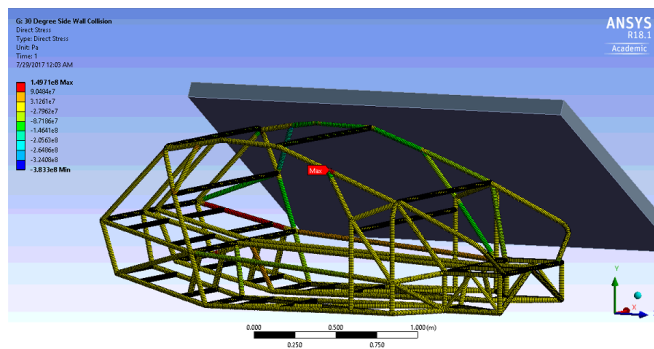


Figure 30: Side 30 degree collision

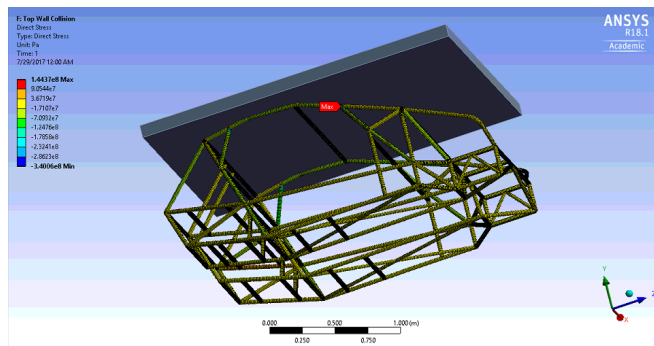


Figure 31: Roof top collision

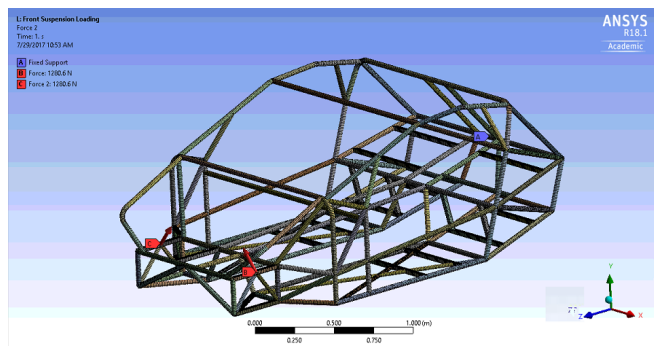


Figure 32: Vehicle rest front subframe loading

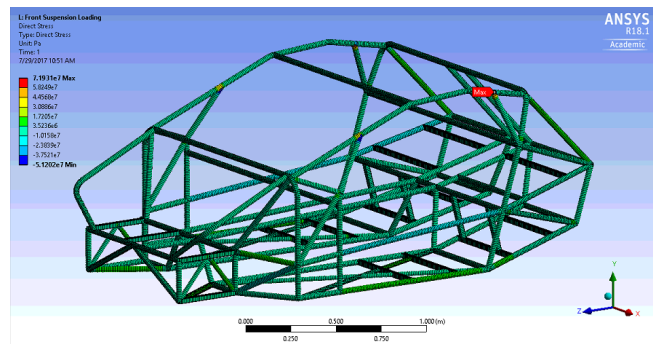


Figure 33: Vehicle rest front subframe stress

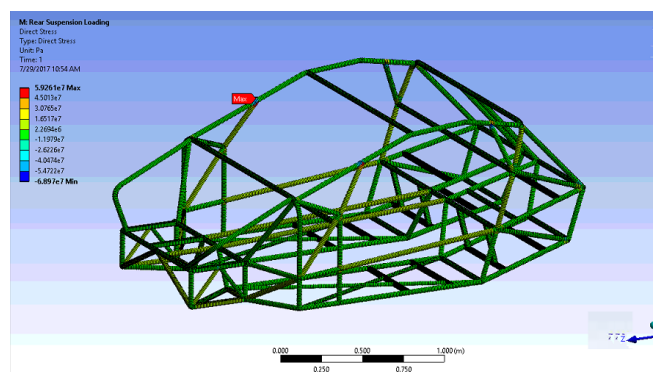


Figure 34: Vehicle rest rear subframe stress

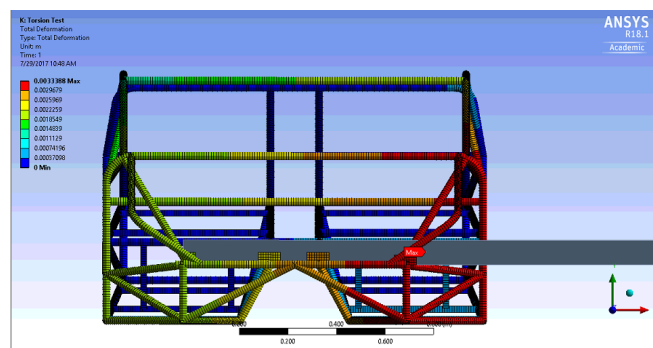


Figure 35: Torsion test, deformation

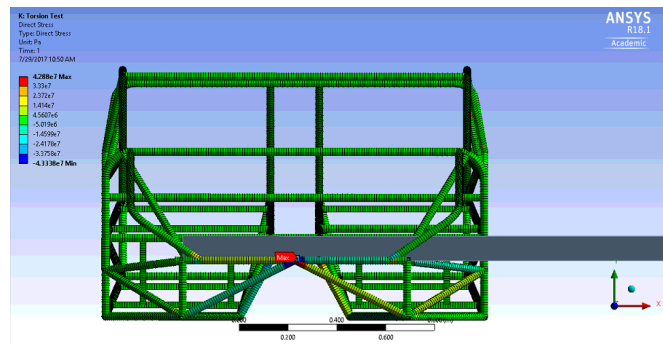


Figure 36: Torsion test, stress

C FEA images for suspension and steering

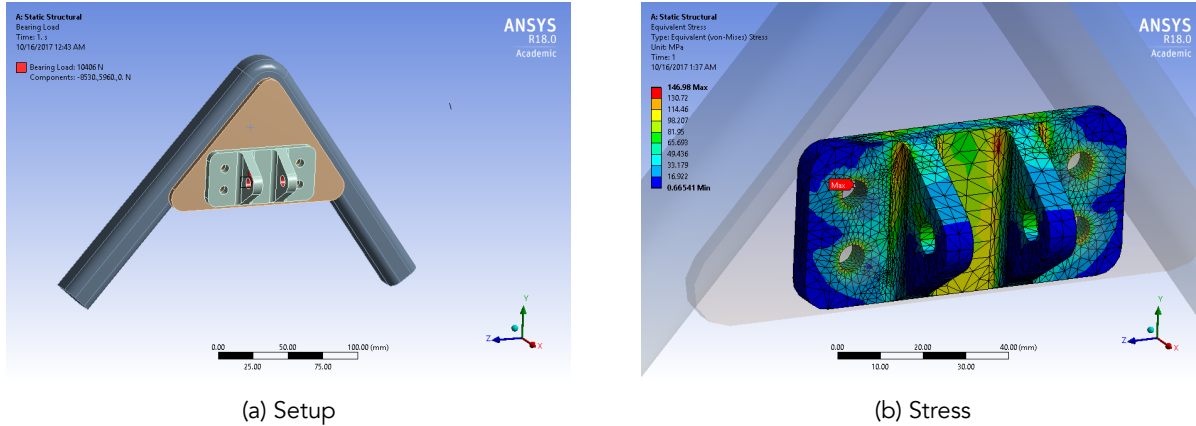


Figure 37: Coilover clevis

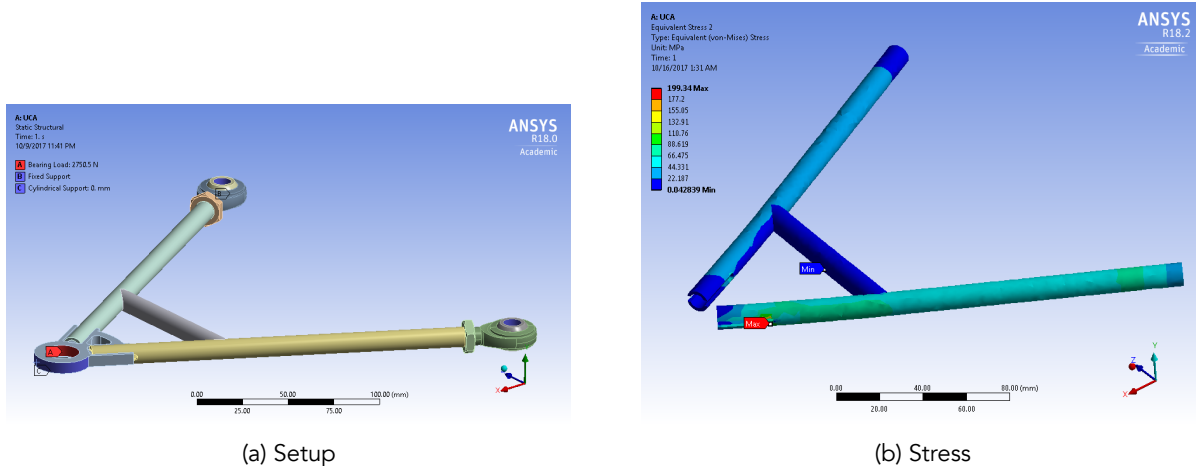


Figure 38: Upper control arm

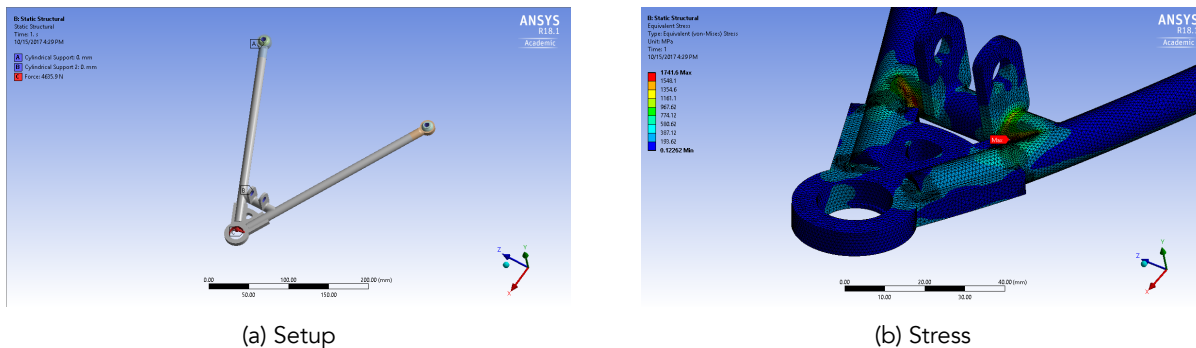


Figure 39: Lower control arm

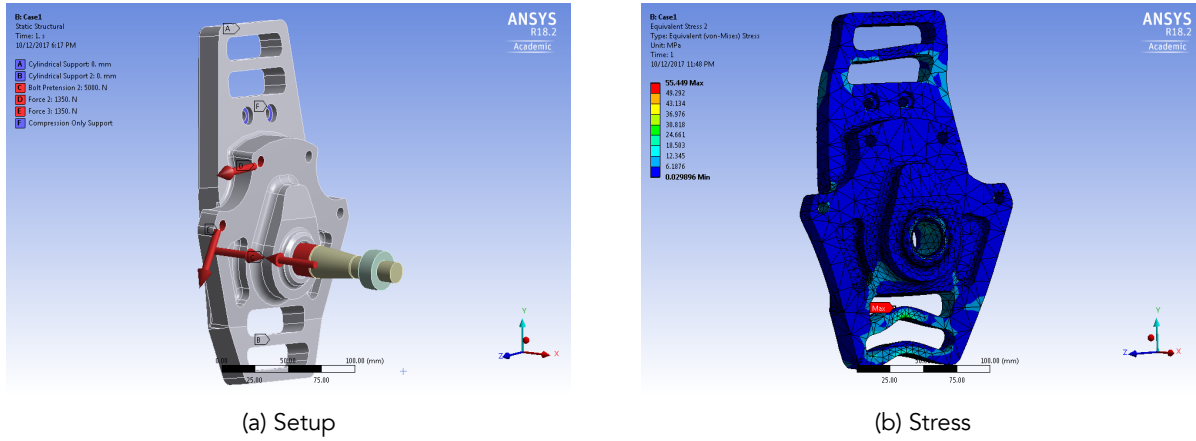


Figure 40: Upright

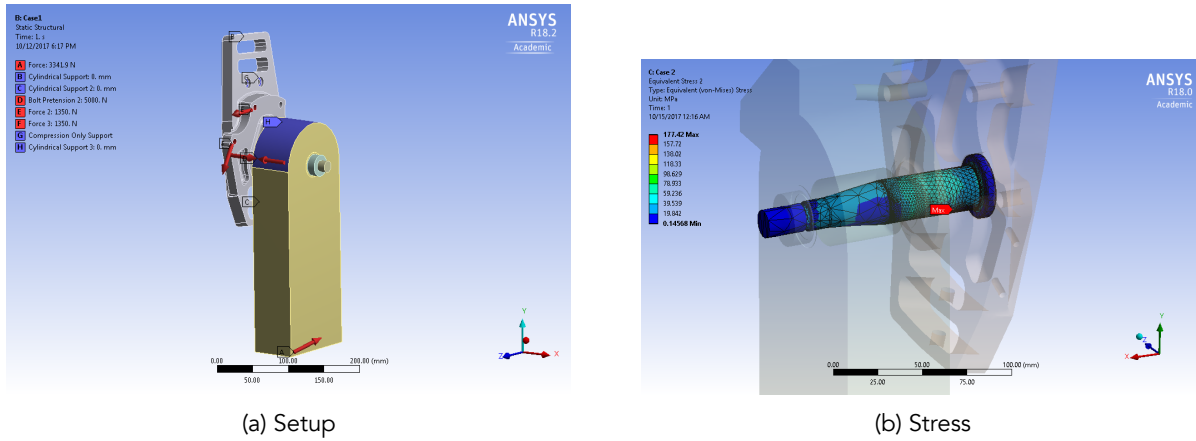


Figure 41: Spindle

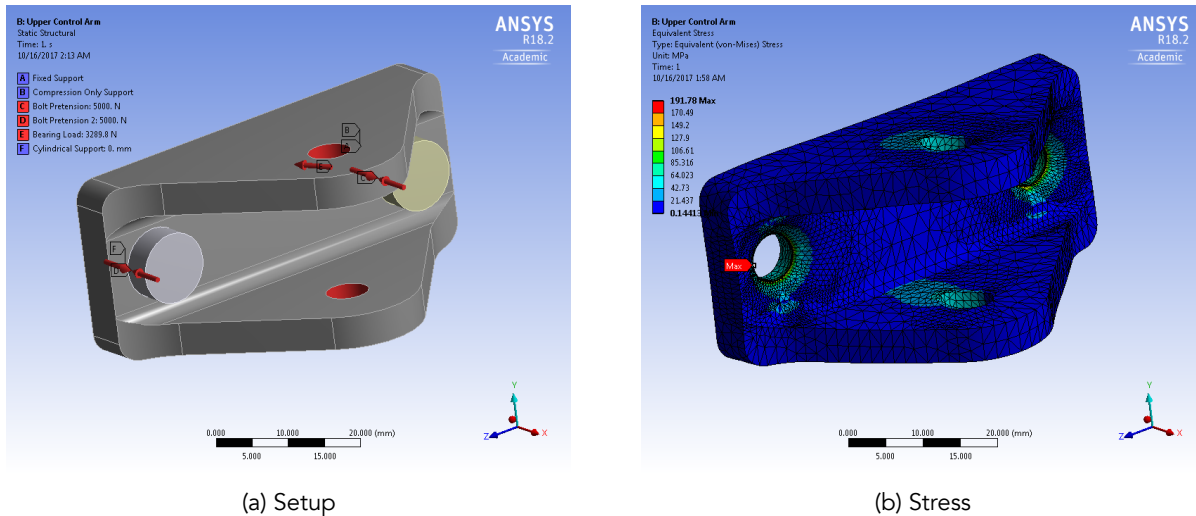


Figure 42: Upper control arm clevis

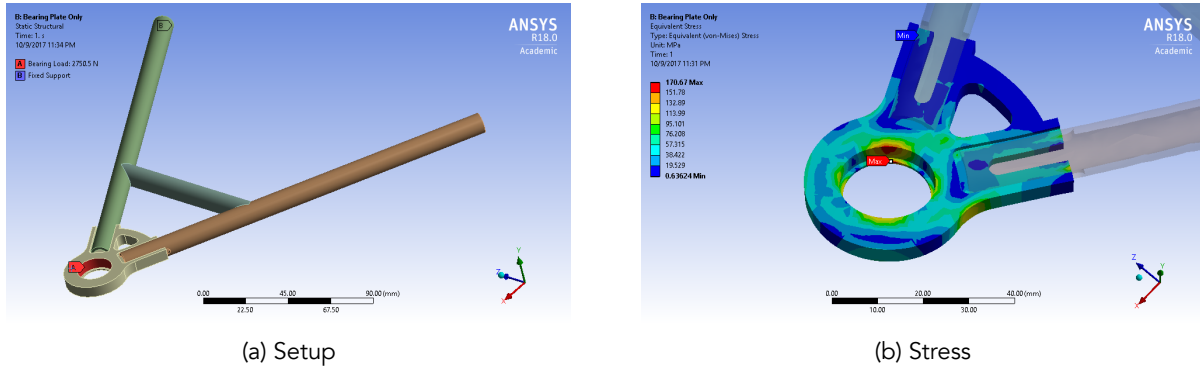


Figure 43: Upper bearing plate

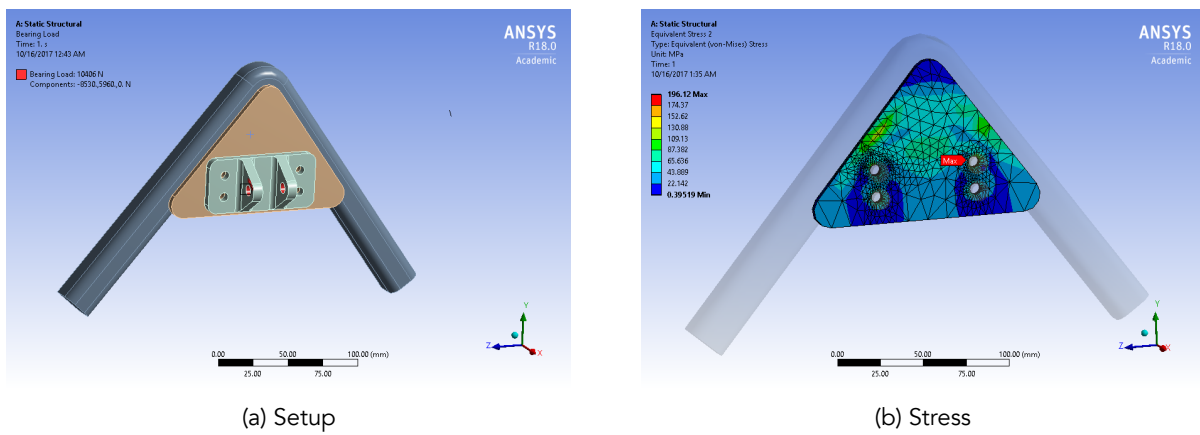


Figure 44: Coilover mounting plate

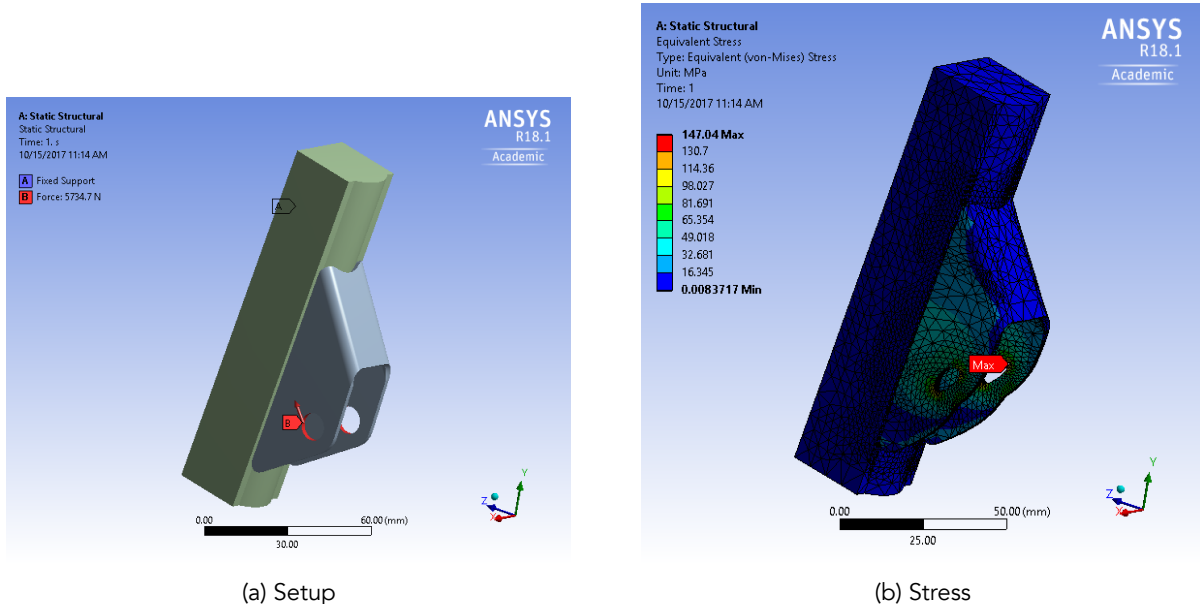


Figure 45: Rear suspension coilover tab

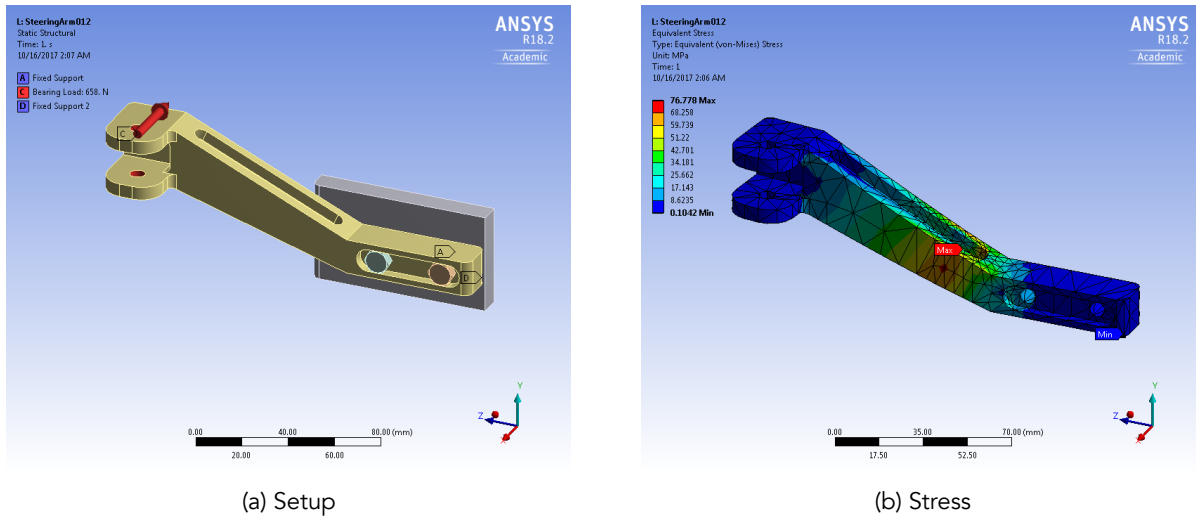


Figure 46: Steering arm

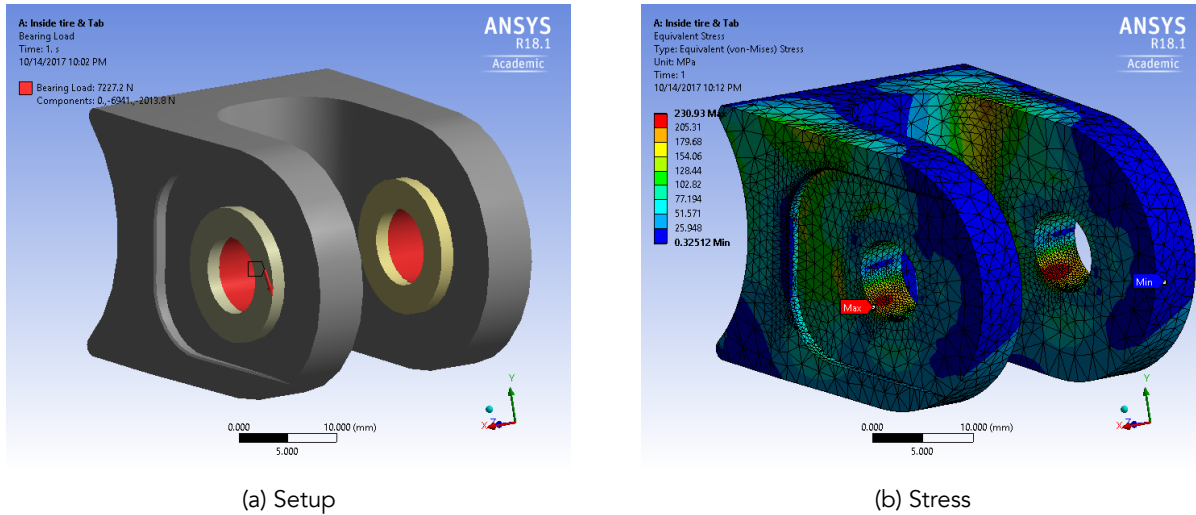


Figure 47: Rear suspension clevis

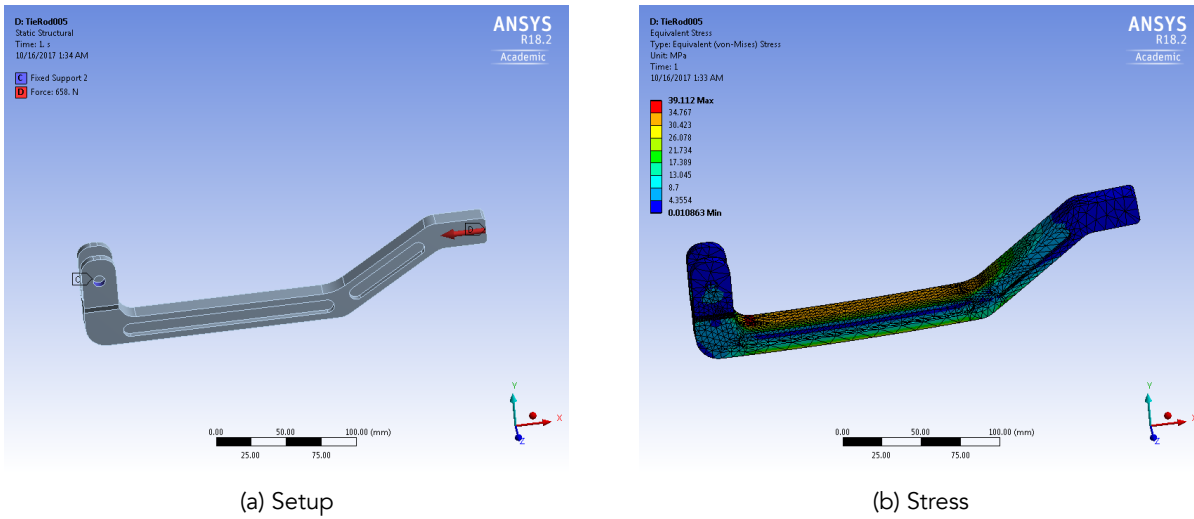


Figure 48: Tie rod

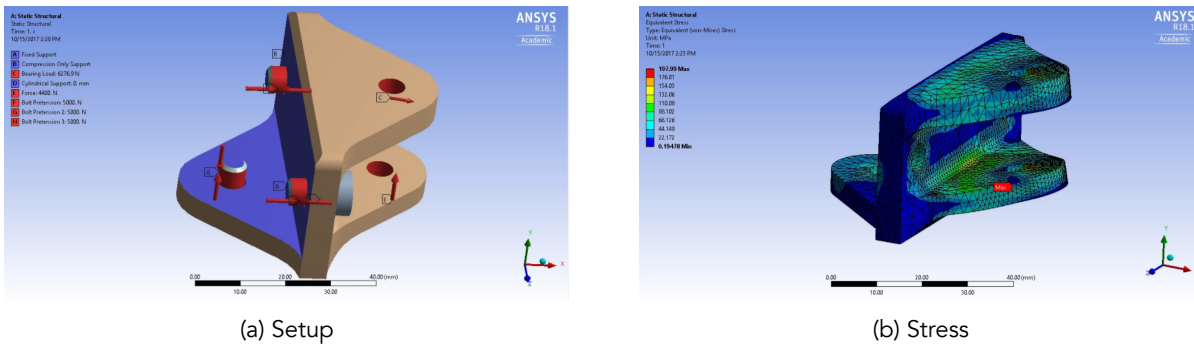


Figure 49: Lower control arm clevis